RCS Rainbow One instruments: Final Report

Prof. Dr Emmanuel J. N. L. Silva

PubMed: https://bit.ly/3PxMZO9

Research Gate: https://bit.ly/44PK3Rt

Prof. Dr Marco A. Versiani

PubMed: https://bit.ly/46a9gah

Research Gate: https://bit.ly/48gnh88

Introduction

In the ever-evolving field of endodontics, nickel-titanium (NiTi) instruments have emerged as a game-changer. These remarkable tools have revolutionized root canal therapy, offering improved efficiency, precision, and patient comfort. NiTi is a remarkable alloy, a blend of nickel and titanium, known for its unique properties. These properties include remarkable flexibility, high fatigue resistance, and the ability to return to its original shape when deformed – the so-called "shape memory" effect. These characteristics have made NiTi instruments the preferred choice for root canal preparation. In the pursuit of understanding NiTi instrument performance, many studies have traditionally employed single-method approaches, focusing on one aspect such as quantitative measurements. While these studies have yielded valuable insights, they have limitations. Single-method studies often overlook the multifaceted nature of NiTi instruments, neglecting qualitative aspects, that may fall short in providing a comprehensive understanding of their performance. Therefore, to truly unlock the capabilities of NiTi instruments, a multimethod research approach is essential.

The multimethod research approach is a methodology that integrates diverse research methods to provide a holistic view of the phenomena under investigation. It marries quantitative and qualitative techniques, promoting triangulation and corroborative evidence. One of its primary advantages is its capacity to enhance research rigor. Traditional single-method studies, while valuable, can be limited in scope and prone to bias. By incorporating qualitative data, researchers can gain a deeper understanding of the practical implications of NiTi instrument use. This can validate and strengthen the findings obtained through quantitative measurements. Another advantage is that the multimethod provides comprehensive insights into NiTi instrument performance. NiTi instrument performance is a multidimensional construct influenced by a plethora of factors, including mechanical properties, metallurgical characterization, and shaping ability. A multimethod approach enables a comprehensive evaluation of these factors, shedding light on the intricate interplay between quantitative and qualitative dimensions. It's not just about measuring physical effects but understanding the practical implications of NiTi instrument use in real clinical scenarios providing a more realistic and actionable view of NiTi instrument performance in the field. Besides, it allows the triangulation, a key principle of the multimethod approach, which involves comparing findings from different methods to validate and corroborate results. In NiTi instrument research, this could mean cross-referencing outcomes obtained through quantitative and qualitative measurements. The convergence of evidence from these diverse sources enhances the validity of research findings and reduces the risk of premature or inaccurate conclusions.

Endodontics is a dynamic field that continually evolves with emerging technologies, materials, and techniques. Embracing the multimethod approach in NiTi instrument research does not just deepen our understanding; it propels the advancement of endodontic practices. By using this comprehensive methodology, researchers can identify nuances and challenges that might have otherwise gone unnoticed. While the multimethod approach offers numerous advantages, it is important to acknowledge the challenges it presents. Conducting a multimethod study demands careful planning, allocation of resources, and expertise in diverse research techniques. Additionally, researchers must ensure the seamless integration of quantitative and qualitative data, avoiding misinterpretation or undue emphasis on one type of data over the other. Moreover, the interpretation of results can be complex when dealing with mixed-method data. Researchers must navigate the intricacies of combining quantitative and qualitative findings to derive meaningful insights.

In summary, NiTi instruments have brought about a paradigm shift in endodontics, enhancing the quality of patient care and clinical practice. However, to harness their full potential, research in this domain must adopt the multimethod approach. This methodology offers a comprehensive understanding of NiTi instrument performance by integrating quantitative and qualitative data, enhancing research rigor, and promoting the evolution of endodontic practices. It is not just about measuring physical outcomes; it is about comprehensively assessing their real-world impact on patients and practitioners. Embracing the multimethod approach is a crucial step toward advancing the field of endodontics and ensuring evidence-based, high-quality dental care for patients. Thus, the present research report aimed to evaluate design, metallurgy, mechanical performance and shaping ability of the following rotary NiTi instruments: RCS Rainbow One 25/0.06 (Ramo Medical, China; Lot 20230606137), Rotate 25/0.06 (VDW, Germany; Lot 385600), Race EVO 25/0.06 (FKG, Switzerland; Lot JE19), One Curve 25/0.06 (MicroMega, France; Lot 739828) and ProTaper Ultimate F2 (Dentsply Sirona, Switzerland; Lot 1751922).

Part I

Design and manufacturing quality

1.1 Background

The mechanical properties of either rotary or reciprocating NiTi instruments for root canal preparation are directly correlated to their design and manufacturing quality. Therefore, the evaluation of these properties is essential to understand their mechanical behavior (**Part II**) as well as their performance during root canal preparation (**Part IV**).

1.2 Aim

To evaluate the design (cross-section, blade, tip) of each instrument and the quality of the machining process (defects along their surface) of RCS Rainbow One 25/0.06 compared to Rotate 25/0.06, Race EVO 25/0.06, One Curve 25/0.06 and ProTaper Ultimate F2.

1.3 Sampling

A total of 15 new 25-mm NiTi instruments were tested regarding their design, as follows:

- -RCS Rainbow One 25/0.06 (n=3)
- -Rotate 25/0.06 (n=3)
- -Race EVO 25/0.06 (n=3)
- -One Curve 25/0.06 (n=3)
- -ProTaper Ultimate F2 (n=3)

1.4 Method

Instruments were evaluated under conventional scanning electron microscopy (SEM) (S-2400, Hitachi, Tokyo, Japan), at ×100 and ×500 magnification, regarding the cross-sectional shape, the symmetry of the blade (symmetric or asymmetric), the presence of surface marks, deformations or defects produced by the machining process, and the geometry of the tip (active or non-active).

1.5 Results

Representative SEM images of tested instruments are depicted in **Figure 1**.

1.5.1 Cross-sectional shape

The examined instruments exhibited varying cross-sectional profiles, and these design disparities could have implications in their mechanical performance. The One Curve instrument, as per the manufacturer's specifications, features distinct cross-sectional zones throughout its length. This design commences with a variable 3-cutting-edge configuration in the initial millimeters (as illustrated in **Figure 1**), transitions through an intermediate zone where the number of cutting edges gradually shifts from 3 to 2 within the middle section, ending in an S-shaped design marked by 2 cutting edges at the coronal level. The other instruments exhibited cross-sectional shapes characterized as parallelogram (ProTaper Ultimate), S-shaped (RCS Rainbow One and Rotate), and triangular (RaCe EVO).

1.5.2 Active blade

In contrast to the other instruments, ProTaper Ultimate displayed a more symmetrical active blade. All other instruments exhibited asymmetrical blades with variable pitch. No radial lands were observed in any of the tested instruments. The surface of ProTaper Ultimate showed black spots throughout its blade possibly due to its thermal treatment.

1.5.3 Quality of the manufacturing process

In terms of surface quality, there were distinct differences among the tested instruments. The highest-quality surface finish was evident in the RaCe EVO, which displayed a smooth appearance with only a limited number of shallow micro-cavities. Following closely, the One Curve instrument exhibited the second-best surface finish, characterized by consistent marks from the grinding manufacturing process. Interestingly, despite the manufacturer's claim of a special heat-treated surface treatment for the RCS Rainbow One instrument, its surface had longitudinal grooves extending throughout its length. Meanwhile, both the Rotate and ProTaper Ultimate instruments displayed surface irregularities stemming from the manufacturing process, accompanied by a few shallow micro-cavities and longitudinal grooves. It is worth noting that the ProTaper Ultimate instrument presented a distinctive feature in the form of barbs on its cutting edge, a characteristic not observed in the other evaluated instruments.

1.5.5 Geometry of the tip

One Curve, RaCe EVO, and Rotate instruments exhibited a subtle rounding of the tip-transition angle, whereas ProTaper Ultimate and RCS Rainbow displayed a more pronounced and well-defined tip angle.

1.5.6 Technical remarks

The paramount factor in determining the success or failure of rotary instruments, regardless of their composition or design, lies in the quality of their manufacturing. Subpar quality control during manufacturing can lead to the development of surface-level microcracks and defects on these instruments. These cracks have the potential to propagate and cause instrument failure at stress levels significantly lower than what they typically encounter during use. Additionally, other defects can create stress concentration points, putting the integrity of the instrument at risk and potentially compromising the success of endodontic procedures. It is important to emphasize that considerably less force is needed to propagate a crack than it takes to initially form one. If these defects are situated in areas experiencing high stress, instrument failure can happen rapidly. The region of greatest stress is typically found along the blade or leading edge of the instrument. To mitigate the formation of microcracks during the initial production of rotary instruments, special surface treatments can be applied. These treatments have the potential to enhance resistance to torque-induced failure, contributing to improved instrument durability and reliability.

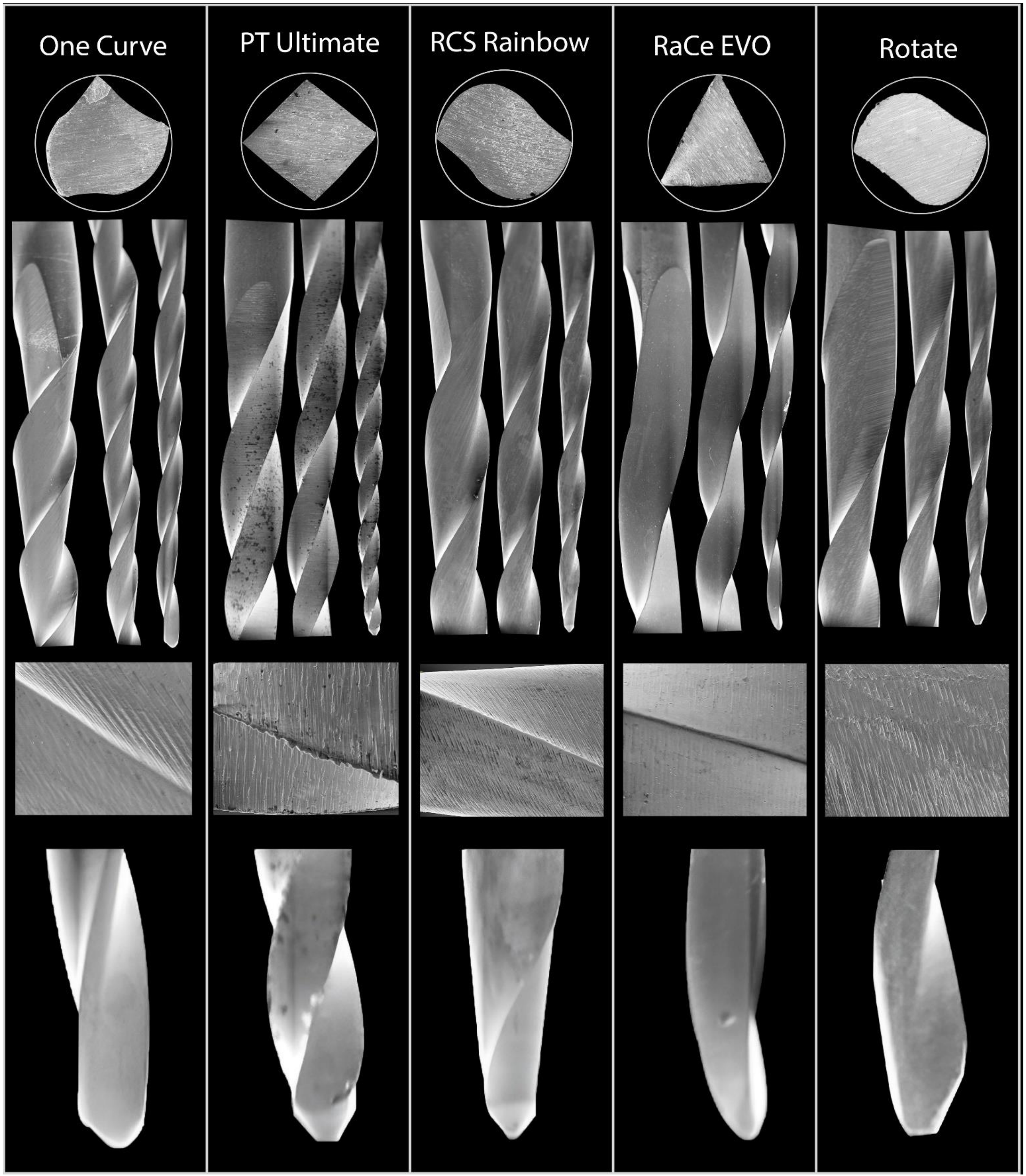

Figure 1. Evaluation of 5 rotary instruments by scanning electron microscopy. From top to bottom: cross-sectional design, active blade at different levels, blade (cutting edge and flute) at higher magnification, and tip geometry.

Part II

Mechanical Testing

2.1 Background

The efficacy of an instrument in removing dentin is contingent upon a complex interplay of various factors related to its design components. These components encompass the number and depth of flutes, cross-sectional area and configuration, helical and rake angles, tip design, metallurgical characteristics, and surface treatments. Within clinical settings, an instrument undergoes cyclic flexural fatigue when it rotates in a curved canal. This is due to the repetitive cycles of compressive and tensile stresses it encounters. On the other hand, torsional failure arises from circumstances such as the entrapment of dentinal chips within machined grooves or the unintended wedging of the instrument's tip against the root canal walls. Both cyclic fatigue and torsional resistance parameters serve as indicators of mechanical strength. Enhancing these parameters holds the promise of improved clinical performance, reducing the likelihood of instrument fractures under these specific stresses. The value of the angle of rotation signifies the ability of an instrument to endure deformation before fracturing under torsional stress. In the clinical context, the bending resistance test plays a pivotal role as it gauges an instrument's flexibility, which correlates with its capacity to withstand cyclic flexural fatigue. Meanwhile, the evaluation of buckling resistance holds paramount importance in clinical applications. This evaluation reveals the ability of an instrument for resisting buckling and maintaining its structural integrity when subjected to compressive forces.[1-16]

2.2 Aim

To evaluate the cyclic fatigue, torsional resistance, cutting ability, bending and buckling resistance of RCS Rainbow One, Rotate, RaCe EVO, One Curve, and ProTaper Ultimate instruments.

2.3 Sampling

Based on the results of previous studies (1-14), a power calculation was performed using G*Power 3.1 (Heinrich Heine University, Dusseldorf, Germany) software indicating a minimum sample size of 10 instruments per group for each test.

2.4 Methods

Before each test, the selected instruments were examined under a stereomicroscope (×13.6 magnification; Opmi Pico, Carl Zeiss Surgical, Germany) looking for defects that would exclude them from being tested, but none was excluded.

2.4.1 Cyclic fatigue

Cyclic fatigue test was performed using a non-tapered stainless steel curved tube apparatus (radius of 6 mm and 86º degree angle) that allows to simulate a instrument working passively in a curved canal, as previously described.[2-15] The tested instruments were adapted to a 6:1 reduction handpiece (Sirona Dental Systems GmbH, Bensheim, Germany) powered by a torque-controlled motor (VDW Silver; VDW GmbH), set with torque according to the manufacturers' directions, and activated at a static position in 400 rpm (**Figure 2**). The electric handpiece was mounted on a device to allow accurate and reproducible placement of each instrument within the simulated canal. The time to fracture was recorded in seconds for each instrument using a digital chronometer and the experiment stop as soon as the fracture was detected visually and/or audibly.

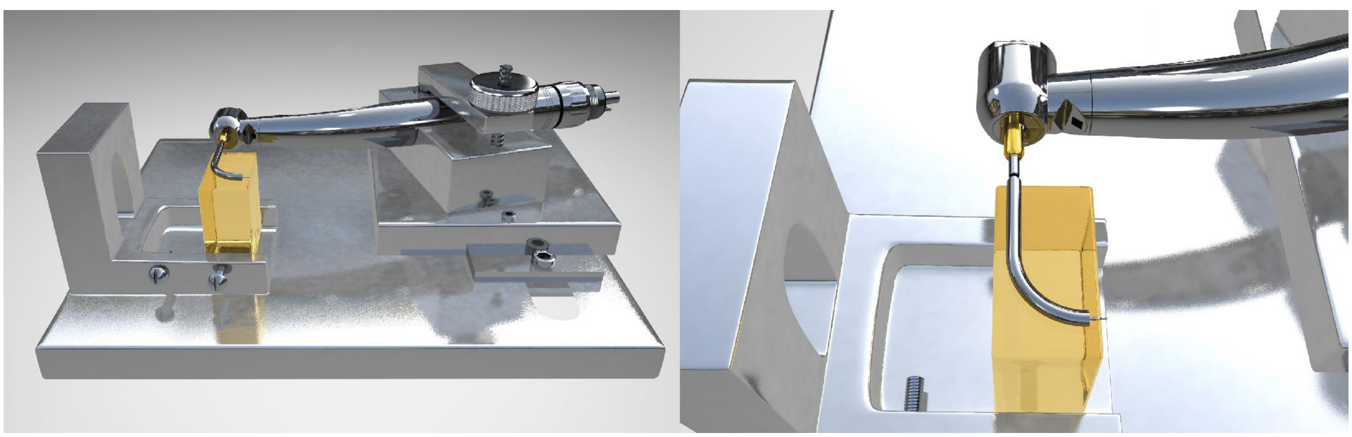

Figure 2. Schematic 3D illustration of the custom-made device to perform cyclic fatigue resistance test.

2.4.2 Torsional resistance

Torsional resistance test was performed at a static torsion model following the ISO 3630-1 specification.[17] Instruments were clamped at their apical 3 mm and rotated counterclockwise at a constant pace of 2 rotations per minute to assess the maximum torque (in N.cm) and the angle of rotation (in degrees) prior to fracture (**Figure 3**) using a torsiometer (model TT100; Odeme Dental Research, Luzerna, Santa Catarina, Brazil) and a dedicated designed software (Odeme TT100; Odeme Dental Research).

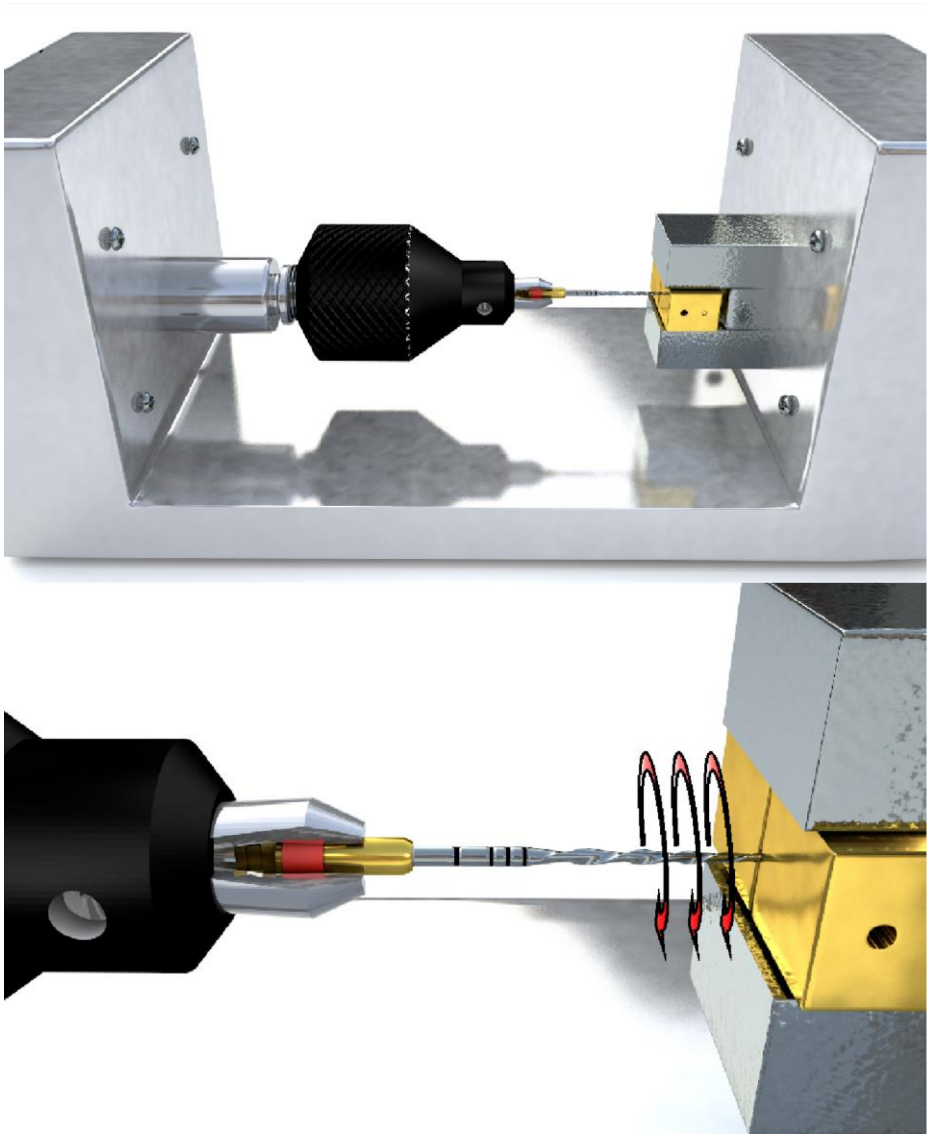

Figure 3. Schematic 3D illustration of the custom-made device used to perform torsional resistance test.

2.4.3 Bending test

The bending resistance test was conducted according to the ISO specifications 3630-1.[17] Instruments were mounted pointing down in a 45º position regarding the floor plane by their grip in the file holder of the motor while having their apical 3 mm attached to a wire linked to a universal testing machine (Instron Corporation 4502; series no H3307, Bucks, England). The test was performed by applying a load of 20 N at a 15-mm/min constant pace until the instrument underwent a displacement of 45º (**Figure 4**). The maximum load required to induce the 45º displacement was recorded in gram-force (gf).

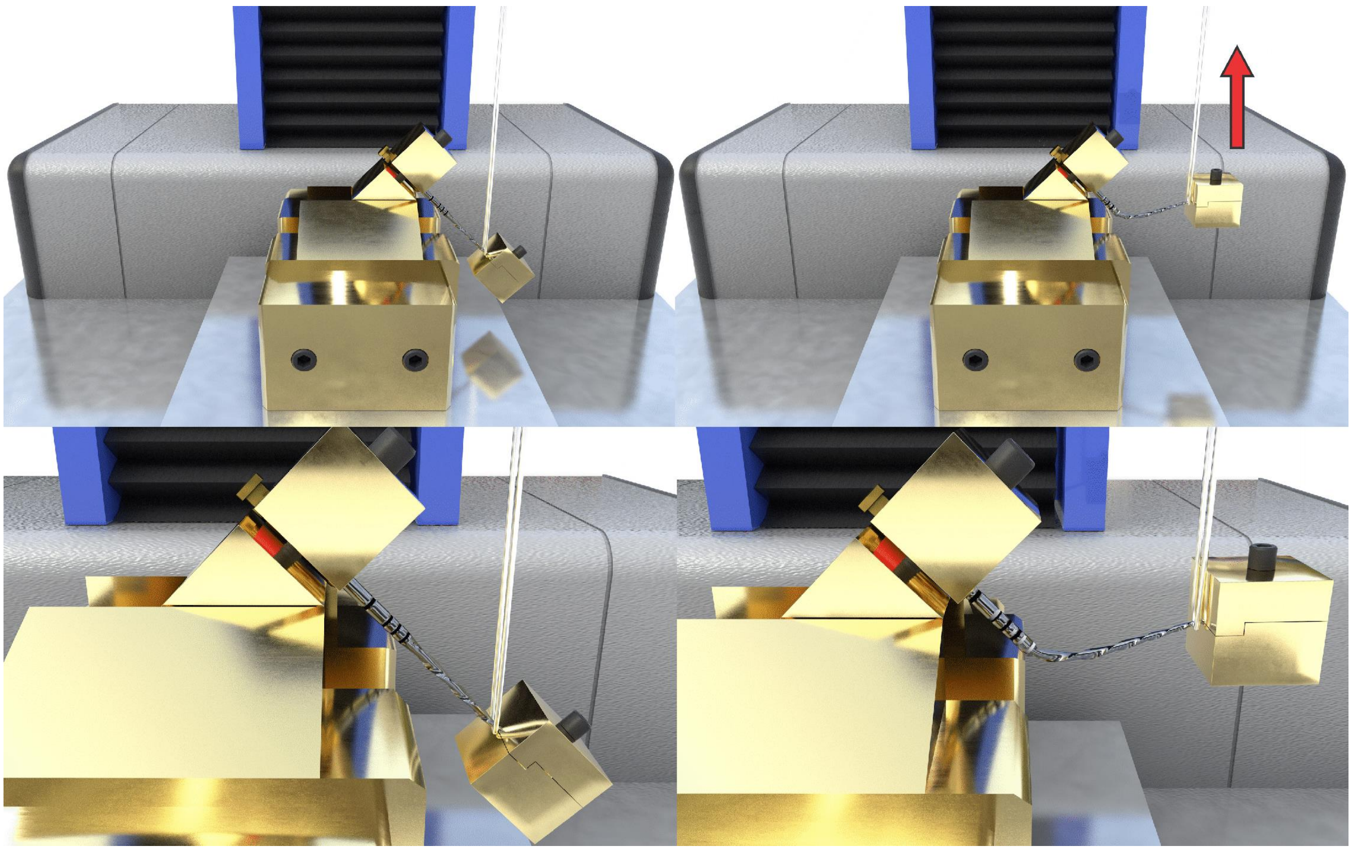

Figure 4. Schematic 3D illustration of the custom-made device used to perform the bending resistance test.

2.4.4 Buckling resistance

For the buckling test, an increasing load was applied in the axial direction of each instrument by using a universal testing machine (Instron Corporation 4502) according to a previous publication.[15] The instrument handle was fixed to the head of the universal testing machine, and the instrument tip was placed in contact with the bottom of a round cavity (1 mm in diameter and 0.5-mm deep) prepared in an aluminum plate. The load (20 N) was applied in the axial direction from the handle to the tip with a speed of 1 mm/min until a lateral elastic (compressive) displacement of 1 mm occurred (**Figure 5**). During the buckling test, it was obtained a diagram of load (N) x deformation (mm) for each instrument. The maximum load needed to induce the elastic displacement of the instrument up to 1 mm was regarded as the buckling resistance of the instrument.

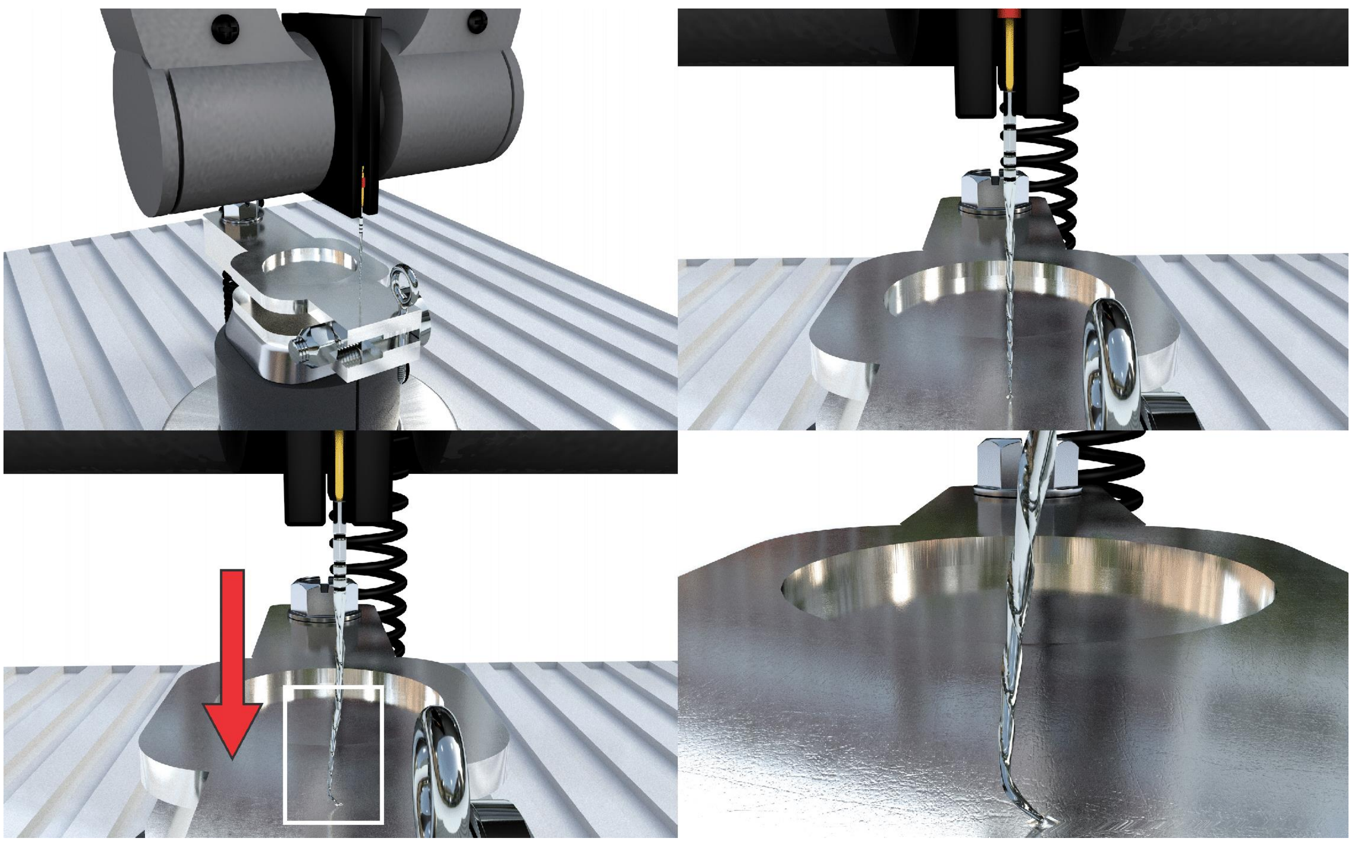

Figure 5. Schematic 3D illustration of the custom-made device used to perform the buckling resistance test.

2.4.5 Cutting ability

A 6:1 reduction handpiece (VDW/Sirona Dental Systems, Bensheim, Germany) powered by an electric motor (Reciproc Silver; VDW GmbH, Munich, Germany) was mounted to a free-falling holder. The holder allowed a free movement in the vertical direction only. The holder was mounted to a linear slide system (Parker Positioning Systems, Parker Hannifin, Cleveland, OH, USA) and the instruments were adjusted in the horizontal direction. The force the mounted handpiece exerted in the vertical direction by its weight is 2.7 N. The head of the handpiece was aligned perpendicularly to a Plexiglass block surface (**Figure 6**). Instruments were tested for their cutting efficiency at 15 mm from the tip. The torque and rotation speed for each instrument were set according to the manufacturers' recommendations. Each instrument was allowed to rotate in direct contact with the Plexiglass block for 1 min. Analysis of the cutting depth in the blocks was performed using a digital caliper with a resolution of 0.01 mm (Mitutoyo, Aurora, IL, USA).

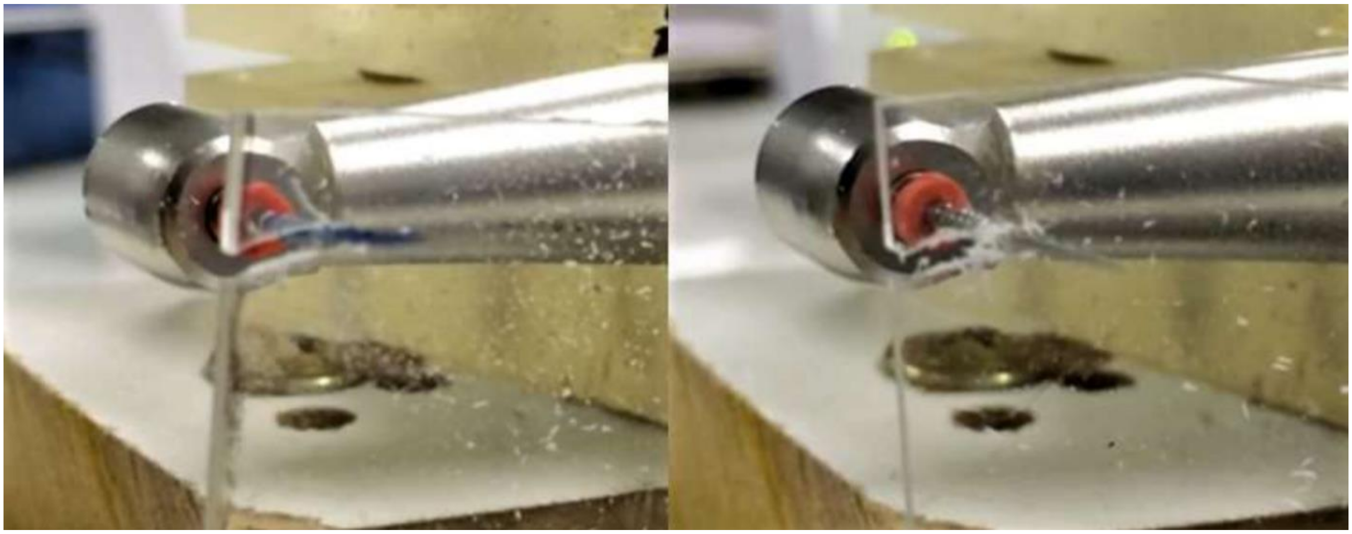

Figure 6. Custom-made device used to perform the cutting ability test.

2.5 Statistical analysis

The results of the mechanical tests were firstly evaluated regarding sample distribution. The Shapiro-Wilk test indicated that the variables "time to failure" ($p=0.166$), "buckling resistance" ($p=0.346$), and "cutting ability" ($p=0.118$) exhibited a normal distribution. Subsequently, group comparisons were conducted using one-way ANOVA, followed by Tukey's post hoc tests. Conversely, the data for "maximum torque to failure" ($p=0.014$), "angle of rotation" ($p=0.001$), and "bending load" ($p=0.016$) did not follow a normal distribution pattern. To analyze these non-normally distributed variables, group comparisons were performed using the Kruskal-Wallis test, followed by Dunn's post hoc tests. The significance level for all statistical analyses was established at 5%. (SPSS v25.0 for Windows; SPSS Inc., Chicago, IL, USA).

2.6. Results

Raw data and statistical analysis regarding the mechanical tests are presented in **Tables 1-6** and **Appendix 1**.

2.6.1 Cyclic fatigue

The highest and lowest mean times to fracture were observed in the One Curve (112.5 ± 11.8 s) and RaCe EVO (51.9 ± 10.4 s) instruments, respectively ($p < 0.05$). RCS Rainbow (86.5 ± 18.7 s) and Rotate (84.4 ± 8.6 s) had intermediate results that were higher than PT Ultimate (68.6 ± 6.3 s) ($p < 0.05$).

Table 1. Mean (standard deviation), median [interquartile range] and range results of time to failure (in seconds) of tested instruments subjected to the cyclic fatigue test. Raw and consolidated data.

RCS Rainbow	Rotate	RaCe EVO	One Curve	PT Ultimate
103	87	70	121	71
89	99	48	91	69
108	86	56	122	82
98	73	46	118	65
92	82	65	125	67
78	98	42	96	70
108	76	47	107	68
58	79	61	124	65
69	84	43	112	57
62	80	41	109	72
86.5 ± 18.7 ^{C}	**84.4 ± 8.6 ^{C}**	**51.9 ± 10.4 ^{A}**	**112.5 ± 11.8 ^{D}**	**68.6 ± 6.3 ^{B}**
90.5 [30.50]	**83.0 [7.5]**	**47.5 [16.0]**	**115.0 [14.3]**	**68.5 [5.3]**
58.0-108.0	**73.0-99.0**	**41.0-70.0**	**91.0-125.0**	**57.0-82.0**

Different superscript letters in the same line mean statistical difference (One-way ANOVA *post hoc* Tukey tests; α=5%)

2.6.2 Torsional resistance

The torque to failure of RCS Rainbow instrument (1.5 ± 0.2 N.cm) was higher than RaCe EVO (1.2 ± 0.3 N.cm) ($p < 0.05$), but similar to the other tested systems ($p > 0.05$). The angle of rotation of RaCe EVO (699.0 ± 131.9º) was significantly higher than RCS Rainbow (546.9 ± 74.6º) and Rotate (555.2 ± 80.2º) ($p < 0.05$), but similar to One Curve (622.3 ± 98.8º) and PT Ultimate (584.2 ± 95.4º) ($p > 0.05$).

Table 2. Mean (standard deviation), median [interquartile range] and range results of torsional test (N.m). Raw and consolidated data.

RCS Rainbow	Rotate	RaCe EVO	One Curve	PT Ultimate
1.3	1.3	1.4	1.5	1.5
1.7	1.5	1.3	1.3	2.4
1.4	1.2	1.1	1.1	1.8
1.5	1.2	1.6	0.8	1.8
1.4	1.4	1.2	1.3	1.5
1.6	1.3	1.5	1.1	1.7
1.9	1.3	0.8	1.5	1.5
1.5	1.5	0.9	1.4	1.3
1.5	1.2	1	1.2	1.2
1.6	1	1.3	1.3	1.3
1.5 ± 0.2 ^{A}	**1.3 ± 0.2 ^{AB}**	**1.2 ± 0.3 ^{BC}**	**1.3 ± 0.2 ^{AC}**	**1.6 ± 0.3 ^{AC}**
1.5 [0.2]	**1.3 [0.2]**	**1.3 [0.4]**	**1.3 [0.3]**	**1.5 [0.4]**
1.3-1.9	**1.0-1.5**	**0.8-1.6**	**0.8-1.5**	**1.2-2,4**

Different superscript letters in the same line mean statistical difference (Kruskal-Wallis *post hoc* Dunn tests; α=5%)

Table 3. Mean (standard deviation), median [interquartile range] and range results of angle of rotation (in º) of tested instruments subjected to the torsional test. Raw and consolidated data.

RCS Rainbow	Rotate	RaCe EVO	One Curve	PT Ultimate
483	593	695	527	531
636	597	705	693	610
598	558	609	608	722
485	462	602	559	624
440	441	664	612	612
534	430	600	523	642
633	591	748	773	684
524	620	634	795	536
493	612	686	546	431
643	648	1047	587	450
546.9 ± 74.6 ^{A}	**555.2 ± 80.2 ^{A}**	**699.0 ± 131.9 ^{B}**	**622.3 ± 98.8 ^{AB}**	**584.2 ± 95.4 ^{AB}**
529.0 [137.3]	**593.0 [122.3]**	**675.0 [87.3]**	**597.5 [123.5]**	**611.0 [105.3]**
440.0-643.0	**430.0-648.0**	**600.0-1047.0**	**523.0-795.0**	**431.0-722.0**

Different superscript letters in the same line mean statistical difference (Kruskal-Wallis *post hoc* Dunn tests; α=5%)

2.6.3 Bending load

The maximum bending load of PT Ultimate (257.8 ± 18.3 gf) was significantly lower than RCS Rainbow (397.4 ± 32.4 gf), Rotate (325.9 ± 21.8 gf), and One Curve (357.7 ± 38.2 gf) ($p < 0.05$), but it was similar to RaCe EVO (260.9 ± 20.4 gf) ($p > 0.05$). These means that the most flexible instruments were PT Ultimate and RaCe EVO.

Table 4. Mean (standard deviation), median [interquartile range] and range results of maximum load (in gf) of tested instruments subjected to the bending test. Raw and consolidated data.

RCS Rainbow	Rotate	RaCe EVO	One Curve	PT Ultimate
404	301	239	331	265
395	294	282	326	251
344	292	247	325	227
415	348	276	418	228
382	336	240	412	282
436	335	266	406	277
347	343	257	347	261
417	334	289	340	257
397	329	233	340	267
437	347	280	332	263
397.4 ± 32.4 ^{A}	**325.9 ± 21.8 ^{AB}**	**260.9 ± 20.4 ^{BC}**	**357.7 ± 38.2 ^{A}**	**257.8 ± 18.3 ^{C}**
400.5 [31.3]	**334.5 [33.3]**	**261.5 [37.3]**	**340.0 [60.0]**	**262.0 [14.0]**
344.0-437.0	**292.0-348.0**	**233.0-289.0**	**325.0-418.0**	**227.0-282.0**

Different superscript letters in the same line mean statistical difference (Kruskal-Wallis *post hoc* Dunn tests; α=5%)

2.6.4 Buckling resistance

The lowest buckling resistance values were observed in RaCe EVO (174.4 ± 25.2 N), while the highest values were observed in PT Ultimate (280.5 ± 25.2 N) and RCS Rainbow (286.7 ± 25.3 N) instruments ($p < 0.05$). Rotate (217.5 ± 20.4 N) and One Curve (252.9 ± 20.2 N) presented intermediate values.

Table 5. Mean (standard deviation), median [interquartile range] and range results of maximum load (in N) of tested instruments subjected to the buckling test. Raw and consolidated data.

RCS Rainbow	Rotate	RaCe EVO	One Curve	PT Ultimate
327	210	155	282	309
268	193	147	276	307
306	236	198	280	277
282	225	169	261	241
263	232	202	233	263
257	220	182	245	255
323	242	196	234	275
275	236	155	231	265
298	196	204	242	311
268	185	136	245	302
286.7 ± 25.3 ^{D}	**217.5 ± 20.4 ^{B}**	**174.4 ± 25.2 ^{A}**	**252.9 ± 20.2 ^{C}**	**280.5 ± 25.2 ^{C,D}**
278.5 [36.0]	**222.5 [35.5]**	**175.5 [42.5]**	**245.0 [36.3]**	**276.0 [42.3]**
257.0-327.0	**185.0-242.0**	**136.0-204.0**	**231.0-282.0**	**241.0-311.0**

Different superscript letters in the same line mean statistical difference (One-way ANOVA *post hoc* Tukey tests; α=5%)

2.6.5 Cutting ability

The lowest and highest cutting ability were observed in the RaCe EVO (4.5 ± 0.8 mm) and One Curve (8.4 ± 1.0 mm) instruments, respectively ($p < 0.05$). The other tested instruments showed intermediate values.

Table 6. Mean (standard deviation), median [interquartile range] and range results of cutting depth (in mm) of tested instruments subjected to the cutting test. Raw and consolidated data.

RCS Rainbow	Rotate	RaCe EVO	One Curve	PT Ultimate
8.7	8.5	4.4	8.7	6.4
8.0	7.9	3.6	9.8	6.1
6.7	8.1	3.2	7.0	6.0
7.2	6.7	4.3	7.4	7.3
7.1	6.9	5.0	8.2	7.0
6.7	7.0	5.3	9.0	6.7
7.0	8.3	3.9	7.7	8.2
6.3	8.0	5.7	7.4	6.7
8.1	7.5	4.9	9.2	7.4
5.6	6.9	4.3	9.3	7.7
7.1 ± 0.9 ^{B}	**7.6 ± 0.7 ^{B,C}**	**4.5 ± 0.8 ^{A}**	**8.4 ± 1.0 ^{C}**	**7.0 ± 0.7 ^{B}**
7.1 [1.1]	**7.7 [1.2]**	**4.4 [1.0]**	**8.5 [1.7]**	**6.9 [0.9]**
5.6-8.7	**6.7-8.5**	**3.2-5.7**	**7.0-9.8**	**6.0-8.2**

Different superscript letters in the same line mean statistical difference (One-way ANOVA *post hoc* Tukey tests; α=5%)

2.7. Remarks

In terms of cyclic fatigue (**Table 1**) and cutting ability (**Table 6**), the Rainbow RCS instruments exhibited intermediate performance. They demonstrated a notably high maximum torque to failure (**Table 2**); however, simultaneously, they exhibited a low angle of rotation (**Table 3**). Among the instruments subjected to testing, the Rainbow RCS displayed the least flexibility (**Table 4**) but showcased a high buckling resistance (**Table 5**). Explanation for these results will be provided after the evaluation of the metallurgical properties of the instruments.

Part III

Metallurgy

3.1 Background

Knowledge of the metal alloy composition and phase transformation temperatures of NiTi instruments are of utmost importance to explain differences in their mechanical performance.

3.2 Aim

To evaluate metal alloy composition and phase transformation temperatures of RCS Rainbow One, Rotate, Race EVO, OneCurve, and ProTaper Ultimate instruments.

3.3 Sampling

Three instruments from each system were analyzed in each test.

3.4 Methods

Metal alloy composition was evaluated by energy-dispersive X-ray spectroscopy (EDS/SEM), while phase transformation temperatures were evaluated by differential scanning calorimetry (DSC).

3.4.1 EDS/SEM analysis

The semi-quantitative elemental analysis from each tested system was carried out to evaluate the proportions of nickel, titanium, or any other relevant element, using a scanning electron microscope (S-2400; Hitachi) equipped with an energy-dispersive X-ray spectroscopy (EDS) (Bruker Quantax; Bruker Corporation, Billerica, MA) set at 20 kV and 3.1 A. The analysis was performed at a 25-mm distance from the surface (400 μm^2) of each instrument using a dedicated software with ZAF correction (Systat Software Inc., San Jose, CA, USA).[5,9,10]

3.4.2 DSC analysis

Differential scanning calorimetry (DSC) method (DSC 204 F1 Phoenix; Netzsch- Gerätebau GmbH, Selb, Germany) was used to determine the phase transition temperatures of instruments' alloy following the American Society for Testing and Materials guidelines.[18] Fragments of 2 to 3 mm in length (5–10 mg) acquired from the coronal active portion of 2 instruments from each system were exposed to a chemical etching consisting of a mixture of 25% hydrofluoric acid, 45% nitric acid, and 30% distilled water, for 2 minutes. Then, they were mounted in an aluminum pan inside the DSC device, with an empty pan serving as control. Each thermal cycle was performed at a pace of 10 ºC/min with temperatures ranging from -150 ºC to 150 ºC, under gaseous nitrogen atmosphere. Phase transformation temperatures were analyzed by the Netzsch Proteus Thermal Analysis software (Netzsch–Gerätebau GmbH). In each group, DSC test was performed twice to confirm the results.[5,9,10]

3.5 Results

3.5.1 EDS/SEM analysis

The EDS confirmed the NiTi nature of all files with near to equiatomic proportions of nickel and titanium (RCS Rainbow One File: 1.024; Race Evo: 1.016; Rotate: 1.031; One Curve N25: 1.037; ProTaper Ultimate F2: 1.012) without registries of any other relevant metallic element.

3.5.2 DSC analysis

As for the DSC results, the apical, middle and coronal sections of the RCS Rainbow One File multicolored instruments showed the same phase transformation temperatures with R-phase start (Rs) and finish (Rf) temperatures being around 32 ºC and 24 ºC, respectively, and the Austenitic start (As) and finish (Af) ones near to 23 ºC and 40 ºC, respectively (**Figure 7A**). The highest Rs (43.4 ºC) and Rf (29.2 ºC) were observed in the ProTaper Ultimate F2 instruments, while the lowest were documented on the Rotate files (Rs: 24.8 ºC; Rf: 14.2 ºC). When analyzing the cooling DSC curves, all files were in R-phase crystallographic arrangement at room temperature (20 ºC), except for the Rotate files which were in a mixed R-phase with austenitic form. At body temperature (36 ºC), the Rotate, Race Evo and RCS Rainbow One File instruments were all at an Austenitic crystallographic arrangement (**Figure 7B**).

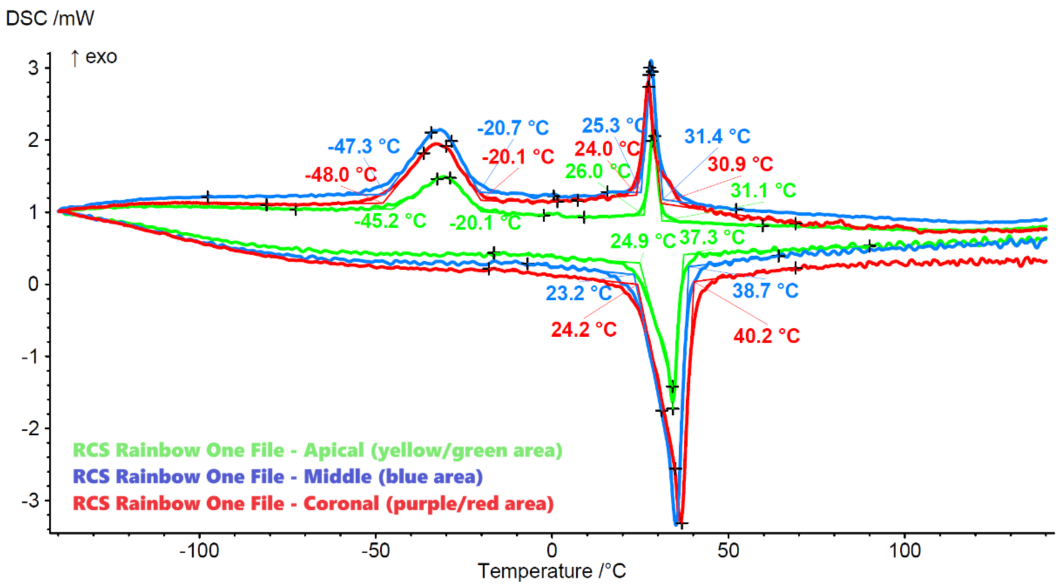

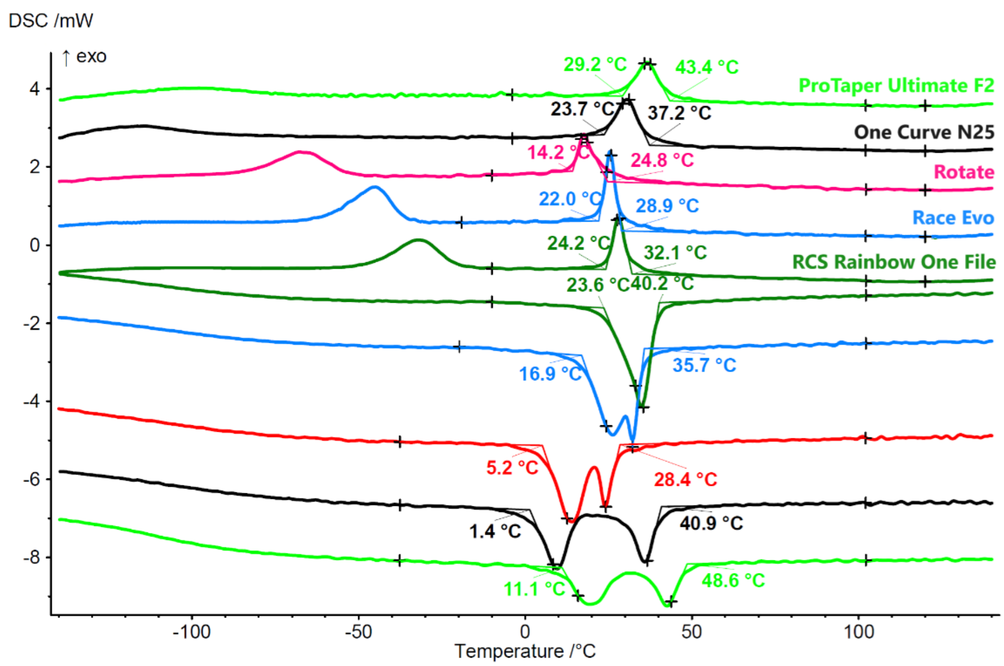

Figure 7. DSC chart showing the phase transformation temperatures of the assessed instruments, with the cooling curves on top (read from right to left) showing the R-phase start (Rs) and finish (Rf) temperatures and heating curves on bottom (read from left to right) detailing the austenitic start (As) and finish (Af) temperatures.

3.6 Remarks

The EDS results confirmed the NiTi equiatomic nature of all tested instruments, without other relevant metallic elements. The first results of the DSC demonstrated that while different color are present in the superficial structure of Rainbow RCS instruments, the three regions (yellow, blue, and red) effectively share the same transformation characteristics. According to the manufacturer, these differences in colorations are related to a diamond-like carbon film. The product is put into a vacuum furnace and passes through the graphite target for solid-state ionization. A thin mist of diamond-like carbon film is sprayed on the surface. Different angles of the workpiece produce different colors. While major differences were observed between the tested instruments, they shared similar transformations characteristics with ProTaper Ultimate F2 being the most martensitic at room temperature and Rotate being the less.

Part IV

Shaping ability

4.1 Background

To simulate clinical usage, this research proposal includes not only the evaluation of the physical properties and metallurgical features of the instruments, but also their shaping ability in the preparation of real root canals using a non-destructive, highly accurate and previous validated analytical tool.

4.2 Aim

To evaluate the unprepared root canal walls in extracted molar teeth using the sequential preparation of RCS Rainbow One, Rotate, Race EVO, One Curve, and ProTaper Ultimate systems by means of micro-CT technology.

4.3 Sampling and sequence protocols

One set of each tested system was used for the preparation of each molar (3 canals) using the following protocols:

- RCS Rainbow One: 17/.08 → 15/.04 → 20/.04 → 25/.06
- Rotate: 15/.04 → 20/.05 → 25/.06
- Race EVO: 15/.04 → 25/.04 → 25.06
- One Curve: 25/.09 (OneFlare) → 14/.03 (OneG) → 25/.06 (OneCurve)
- ProTaper Ultimate: 16/.02v (Slider) → 20/.04v (Shaper) → 20/.07v (F1) → 25/.08 (F2)

After preparation of all canals using this sequence, the palatal canal was further enlarged using the size 35/.06 instrument of each system, with the exception of ProTaper Ultimate in which the F3 instrument (30/.09) was used.

4.4 Method

Thirty maxillary molars with completely formed roots, no internal resorption, calcification, previous endodontic treatment, or root fracture will be image before preparation at a micro-CT device (SkyScan 1275; Bruker-MicroCT, Kontich, Belgium) adjusted with standardized scanning and reconstruction parameters, according to previous studies.[11,19-23] After reconstruction using standardized parameters (NRecon v.1.6.9; Bruker-microCT), root canal configuration was evaluated in each specimen and preoperative parameters (length, volume, and surface area) (**Table 7**) of each main root canal were calculated (CTAn v.1.14.4; Bruker-microCT). The specimens was then anatomically matched to create 5 groups of 5 teeth (n=15 canals per group), according to the preparation systems. After root canal preparation, the specimens were submitted to a second scan and reconstruction procedures following the previously mentioned parameters. Datasets acquired before and after preparation were co-registered (aligned) and evaluated quantitatively regarding the percentage of the untouched canal walls (unprepared surface areas) determined by the formula $(A_u/A_b)*100$, where A_u and A_b represent the unprepared area and the canal area before preparation, respectively. Quantitative analysis also included percentage variation of the morphometric parameters of volume and surface area.

Table 7. 3D parameters of root canals evaluated before and after preparation (shaping ability).

Parameters	Description / Meaning
Volume	The amount of space occupied by a three-dimensional object (root canal) as measured in cubic units (mm^3) within the volume of interest (VOI). Root canal contours were semi-automatically outlined on the loaded images, and the pixels contained within the contour boundaries were considered for the VOI statistics. After root canal preparation it is expected an increase in the original volume of the root canal. As much canal volume increases as much space for disinfection and obturation procedures is created; however, excessive removal of dentin may compromise tooth structure which may lead to root fracture.
Surface Area	For the measurement of the surface area of the three-dimensional multilayer data set (in mm^2), two components to surface measured in a two-dimensional plane were used; first the perimeters of the binarized objects on each cross-sectional level and second the vertical surfaces exposed by pixel differences between adjacent cross sections. Original root canal walls are irregular. Preparation of its surface area allows for a better sealing of the canal space by obturation materials. In some instances, the irregularities of the surface area is so high that its measurement after preparation may have a low value than before preparation.
Unprepared Area (Untouched canal walls)	The measurement of this parameter is based on the superimposition of the root canal outline (surface area) before and after preparation. The unprepared area is considered the surface area of the root canal not included within the canal area after preparation. The area of untouched canal surface was determined by calculating the number of static voxels (voxels present in the same position on the canal surface before and after instrumentation). The untouched area was expressed as a percentage of the total number of voxels present on the canal surface, i.e. the surface area of the root canal in which the instrument did not touch. Although the main canal and minor anatomic irregularities are generally incorporated into preparation, even areas of the main root canal have been shown to remain untouched by instruments. These areas may harbour bacterial biofilm which may be responsible for treatment failure. Thus, as much root canal walls the instrument touches as much biofilm removal is expected.

The surface of pre- and post-operative models of root canal were textured in different colors to allow the qualitative comparison among groups.

4.5 Statistical analysis

The Shapiro-Wilk and Levene tests were used to evaluate the assumption of normality and the equality of variance of data sets. Based on the data distribution (Shapiro-Wilk test), results were presented as mean (standard deviation) or median (interquartile range) and statistically compared among groups using One-Way ANOVA or Kruskall-Wallis tests. Significance level was set at $p < 0.05$ (SPSS v25.0 for Windows; SPSS Inc., Chicago, IL, USA).

4.6 Results

Statistical analyses are reported in **Figures 8 to 12** (raw data) and **Table 8**. **Figure 13** shows representative micro-CT 3D models of the prepared specimens, depicting the superimposed root canal system before (in yellow) and after (in purple) preparation procedures.

			Before		After		% Untouched Walls
Sample	Canal	Length	Volume	Surface Area	Volume	Surface Area	
1	DB	5,86	0,65	10,02	1,75	14,96	16,20
1	MB	7,48	0,39	7,03	1,82	14,85	25,50
1	P	8,16	2,58	22,11	3,38	24,37	18,92
5	DB	9,22	1,50	14,97	3,20	22,74	20,50
5	MB	10,26	1,27	16,33	3,14	24,05	20,10
5	P	9,52	5,35	36,90	7,07	37,33	17,94
10	DB	7,22	1,14	12,10	2,22	16,62	9,77
10	MB	7,98	4,50	31,57	4,83	32,47	32,23
10	P	8,92	6,27	31,94	6,67	33,25	32,40
20	DB	7,78	1,95	16,32	2,39	18,04	36,51
20	MB	8,28	3,30	38,45	4,55	40,56	68,56
20	P	7,88	3,18	20,66	3,34	21,26	55,19
26	DB	8,84	0,90	11,99	2,69	20,02	14,30
26	MB	8,24	0,76	11,92	2,63	20,32	15,16
26	P	9,7	3,75	25,00	4,22	26,32	39,97

Figure 8. Micro-CT raw data of maxillary molar canals prepared with the Rotate system.

			Before		After		% Untouched Walls
Sample	Canal	Length	Volume	Surface Area	Volume	Surface Area	
2	DB	7,28	2,69	20,43	3,56	22,72	31,93
2	MB	8,1	3,71	43,31	4,89	46,11	69,36
2	P	10,72	8,34	39,69	8,68	40,57	38,34
7	DB	6,5	1,07	12,51	1,93	15,77	23,91
7	MB	6,5	1,20	14,12	2,16	18,27	33,52
7	P	6,24	3,06	17,76	3,29	18,70	35,49
13	DB	10,08	2,52	20,71	3,73	24,81	14,92
13	MB	12,14	5,17	41,86	6,92	45,07	43,38
13	P	12,78	6,13	34,94	7,51	39,59	31,22
22	DB	6,58	3,41	22,66	3,80	23,84	31,15
22	MB	7,48	4,71	34,69	5,62	38,92	34,05
22	P	7,32	8,31	34,60	8,44	35,03	37,69
25	DB	7,98	2,72	19,12	3,17	20,80	12,82
25	MB	7,62	1,43	16,93	2,28	20,21	33,41
25	P	9,18	8,19	37,56	8,24	37,62	63,89

Figure 9. Micro-CT raw data of maxillary molar canals prepared with the ProTaper Ultimate system.

			Before		After		% Untouched Walls
Sample	Canal	Length	Volume	Surface Area	Volume	Surface Area	
3	DB	6	1,22	11,31	1,77	13,81	14,88
3	MB	7,34	3,73	31,47	4,51	32,38	45,15
3	P	4,94	1,60	11,74	1,85	13,19	37,26
9	DB	8,28	1,20	13,22	2,70	19,41	24,92
9	MB	9,36	4,44	32,62	5,36	35,05	64,92
9	P	7,32	4,60	24,41	5,06	26,28	60,12
15	DB	7,16	4,81	30,89	5,59	31,12	16,72
15	MB	7,08	6,68	48,83	7,14	49,35	64,36
15	P	6,5	11,49	42,93	11,68	43,46	51,31
21	DB	7,44	0,88	11,20	2,81	19,90	2,11
21	MB	7,98	2,25	21,42	3,85	26,53	29,48
21	P	9,62	4,70	27,79	5,08	29,05	18,20
23	DB	6,88	2,93	20,21	3,54	22,33	22,24
23	MB	7,06	6,30	36,43	6,74	36,88	45,00
23	P	7,18	5,83	27,48	6,23	28,53	25,89

Figure 10. Micro-CT raw data of maxillary molar canals prepared with the RaCe system.

			Before		After		% Untouched Walls
Sample	Canal	Length	Volume	Surface Area	Volume	Surface Area	
4	DB	8,5	1,49	14,34	3,01	20,35	20,70
4	MB	7,76	1,31	16,36	2,76	21,50	32,33
4	P	7,66	2,50	18,20	3,19	20,80	32,40
16	DB	10,42	0,89	13,24	3,68	24,36	12,15
16	MB	9,42	1,81	21,94	4,17	29,35	35,69
16	P	8,5	1,53	29,78	3,83	37,07	59,55
17	DB	8,48	1,64	15,82	3,04	20,92	23,50
17	MB	9,7	2,78	32,40	4,63	37,30	53,56
17	P	9,46	4,99	32,34	5,66	35,40	11,16
18	DB	11,36	3,88	35,84	7,00	45,23	34,10
18	MB	11,26	4,58	55,45	7,76	62,82	63,45
18	P	12,32	6,02	37,41	8,08	43,26	15,00
29	DB	8,12	1,82	16,07	3,14	20,85	13,49
29	MB	8,36	2,97	27,16	4,11	30,24	38,66
29	P	9,38	3,77	24,83	4,47	27,12	15,69

Figure 11. Micro-CT raw data of maxillary molar canals prepared with the One Curve system.

			Before		After		% Untouched Walls
Sample	Canal	Length	Volume	Surface Area	Volume	Surface Area	
12	DB	11,56	1,95	19,62	5,53	32,37	9,89
12	MB	12,18	3,10	26,98	5,68	34,42	24,85
12	P	10,94	5,01	30,59	5,91	33,17	32,51
14	DB	8,42	0,62	10,46	3,00	20,44	18,50
14	MB	9,36	1,13	18,90	4,15	27,23	26,05
14	P	9,68	2,05	20,56	4,15	26,68	4,80
19	DB	8,38	3,06	26,29	4,26	28,70	45,12
19	MB	8,48	2,26	30,76	3,96	36,49	56,46
19	P	9,8	5,98	36,07	7,07	39,58	18,27
24	DB	8,68	1,03	12,23	2,73	19,07	15,30
24	MB	9,16	2,34	26,64	3,84	30,36	52,20
24	P	8,56	2,16	17,76	3,08	20,93	29,19
30	DB	6,6	1,07	14,96	2,06	16,43	31,40
30	MB	7	2,09	21,85	2,79	22,92	59,54
30	P	5,82	3,49	20,26	3,63	20,69	45,07

Figure 12. Micro-CT raw data of maxillary molar canals prepared with the RCS Rainbow One system.

Table 8. Length (in mm), volume (in mm^3), surface area (in mm^2), and unprepared areas (%) parameters (mean ± standard deviation or median [interquartile range], and range interval) calculated before and after preparation of 75 root canals of maxillary molars with 5 rotary systems (n=15).

		Rotate	PT Ultimate	RaCe EVO	One Curve	RCS Rainbow	*p*-value
Parameters				**Mesiobuccal Canal**			
Canal Length	Before	8.4 ± 1.1 [7.5–10.3]	8.4 ± 2.2 [6.5–12.1]	7.8 ± 1.0 [7.1–9.4]	9.3 ± 1.3 [7.8–11.3]	9.2 ± 1.9 [7.0–12.2]	.542
Volume	Before	2.0 ± 1.8 [0.4–4.5]	3.2 ± 1.8 [1.2–5.2]	4.7 ± 1.8 [2.3–6.7]	2.7 ± 1.3 [1.3–4.6]	2.2 ± 0.7 [1.1–3.1]	.091
	After	3.4 ± 1.3 [1.8–4.8]	4.4 ± 2.1 [2.2–6.9]	5.5 ± 1.4 [3.9–7.1]	4.7 ± 1.9 [2.8–7.8]	4.1 ± 1.0 [2.8–5.7]	.249
Surface Area	Before	21.1 ± 13.4 [7.0–38.5]	30.2 ± 13.8 [14.1–43.3]	34.2 ± 9.9 [21.4–48.8]	30.7 ± 15.1 [16.4–55.5]	25.0 ± 4.7 [18.9–30.8]	.440
	After	26.5 ± 10.2 [14.9–40.6]	33.7 ± 13.5 [18.3–46.1]	36.0 ± 8.4 [26.5–49.4]	36.2 ± 15.9 [21.5–62.8]	30.3 ± 5.5 [22.9–36.5]	.653
Unprepared Area	After	32.3 ± 21.2 [15.2–68.6]	42.7 ± 15.5 [33.4–69.4]	49.8 ± 15.0 [29.5–64.9]	44.7 ± 13.2 [32.3–63.5]	43.8 ± 17.0 [24.9–59.5]	.477
				Distobuccal Canal			
Canal Length	Before	7.8 ± 1.3 [5.9–9.2]	7.7 ± 1.5 [6.5–10.1]	7.2 ± 0.8 [6.0–8.3]	9.4 ± 1.4 [8.1–11.4]	8.7 ± 1.8 [6.6–11.6]	.130
Volume	Before	1.1 [1.0] [0.7–2.0]	2.7 [1.3] [1.1–3.4]	1.2 [2.8] [0.9–4.8]	1.6 [1.7] [0.9–3.9]	1.1 [1.7] [0.6–3.1]	.412
	After	2.4 [1.0] [1.8–3.2]	3.6 [1.2] [1.9–3.8]	2.8 [2.3] [1.8–5.6]	3.1 [2.3] [3.0–7.0]	3.0 [2.5] [2.1–5.5]	.270
Surface Area	Before	12.1 [4.6] [10.0–16.3]	20.4 [5.9] [12.5–22.7]	13.2 [14.3] [11.2–30.9]	15.8 [12.2] [13.2–35.8]	15.0 [11.6] [10.5–26.3]	.329
	After	18.0 [5.6] [15.8–24.8]	22.7 [6.0] [15.8–24.8]	19.9 [10.1] [13.8–31.1]	20.0 [14.2] [20.4–45.2]	20.4 [12.8] [16.4–32.4]	.388
Unprepared Area	After	16.2 [16.5] [9.8–36.5]	23.9 [17.7] [12.8–31.9]	16.7 [15.1] [2.1–24.9]	20.7 [16.0] [12.2–34.1]	18.5 [25.7] [9.9–45.1]	.916
				Palatal Canal			
Canal Length	Before	8.8 ± 0.8 [7.9–9.7]	9.2 ± 2.6 [6.2–12.8]	7.1 ± 1.7 [4.9–9.6]	9.5 ± 1.8 [7.7–12.3]	9.0 ± 1.9 [5.8–10.9]	.300
Volume	Before	4.2 ± 1.5 [2.6–6.3]	6.8 ± 2.3 [3.1–8.3]	5.6 ± 3.6 [1.6–11.5]	3.8 ± 1.8 [1.5–6.0]	3.7 ± 1.7 [2.1–6.0]	.265
	After	4.9 ± 1.8 [3.3–7.1]	7.2 ± 2.2 [3.3–8.7]	6.0 ± 3.6 [1.9–11.7]	5.0 ± 1.9 [3.2–8.1]	4.8 ± 1.7 [3.1–7.1]	.480
Surface Area	Before	27.3 ± 6.9 [20.7–36.9]	32.9 ± 8.7 [17.8–39.7]	26.9 ± 11.1 [11.7–42.9]	28,5 ± 7.3 [18.2–37.4]	25.0 ± 7.9 [17.8–36.1]	.599
	After	28.5 ± 6.6 [21.3–37.3]	34.3 ± 9.0 [18.7–40.6]	28.1 ± 10.8 [13.2–43.5]	32.7 ± 8.8 [20.8–43.3]	28.2 ± 8.2 [20.7–39.6]	.795
Unprepared Area	After	32.9 ± 15.5 [17.9–55.2]	41.3 ± 12.9 [31.2–63.9]	38.6 ± 17.4 [18.2–60.1]	26.8 ± 20.1 [11.2–59.6]	26.0 ± 15.2 [4.8–45.1]	.585

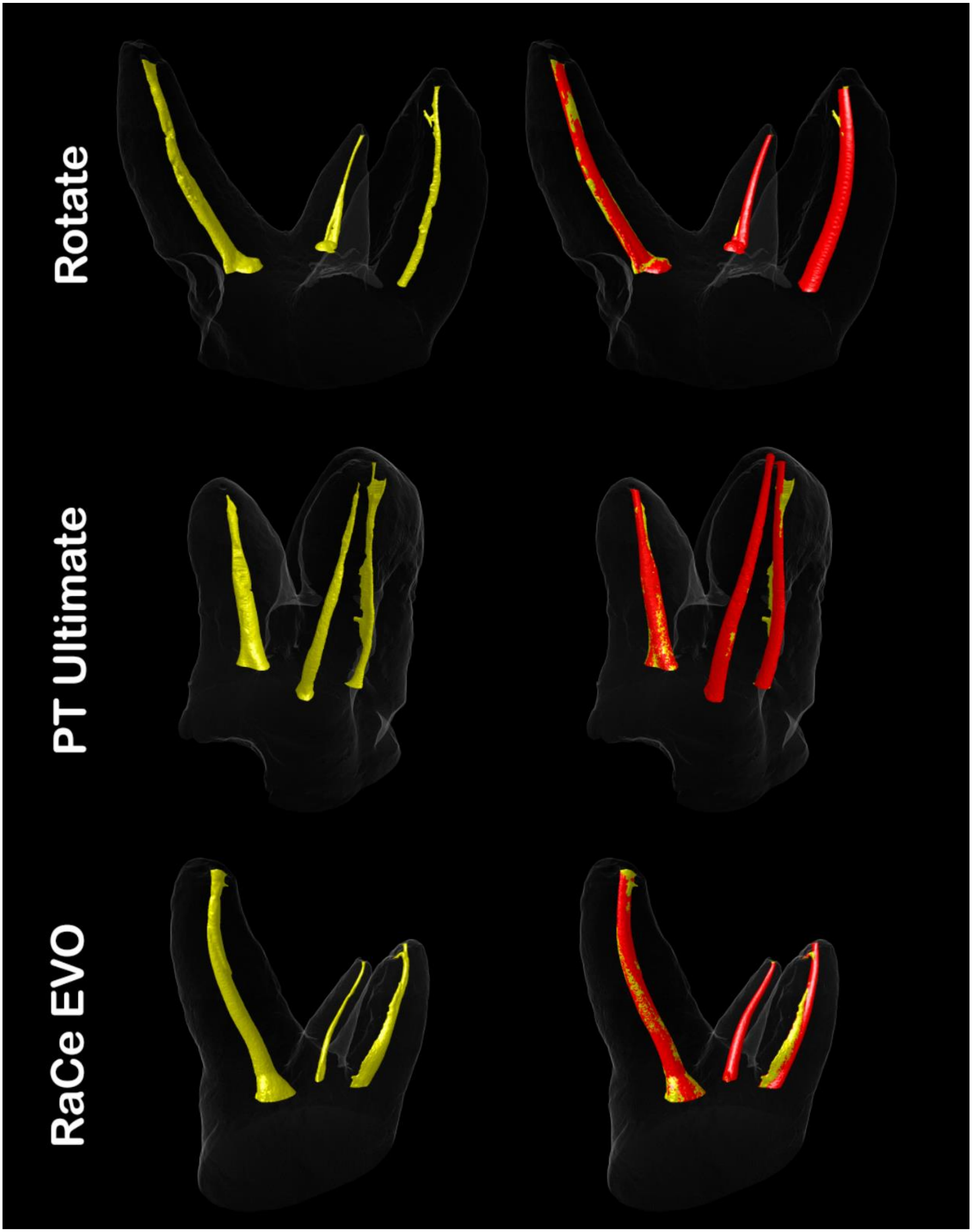
Rotate
PT Ultimate
RaCe EVO

Figure 9. Representative 3D models of root canals of maxillary molars before (in yellow) and after (in red) preparation with 5 rotary systems.

4.7 Remarks

- No difference was observed between shaping ability of 5 NiTi systems tested in this study regarding 3D parameters. This result can be explained by (i) the dimensional similarity of the master apical instruments, (ii) the similar regarding instrument kinematic, and (iii) preliminary efforts to ensure morphological comparability of selected root canals in each group regarding configuration, length, volume, and surface area, enhancing the internal validity of the method and reducing the anatomical bias.
- None of the preparation protocols was able to prepare all surface area of the root canal walls. This result is in accordance with literature and can be explained because of the anatomical irregularities of the root canal system of maxillary molars.
- No instrument fracture (separation) or significant transportation of the original canal pathway were observed.

APPENDIX 1

Table S1. Mean (standard deviation), median [interquartile range] and range results of cyclic fatigue, torsional resistance, bending resistance, buckling resistance, and cutting ability tests of flat and non-flat rotary instruments.

Mechanical tests	Parameters	RCS Rainbow	Rotate	RaCe EVO	One Curve	PT Ultimate
Cyclic fatigue	Time to fracture (s)	86.5 ± 18.7 90.5 [30.50] 58.0-108.0	84.4 ± 8.6 83.0 [7.5] 73.0-99.0	51.9 ± 10.4 47.5 [16.0] 41.0-70.0	112.5 ± 11.8 115.0 [14.3] 91.0-125.0	68.6 ± 6.3 68.5 [5.3] 57.0-82.0
Torsional resistance	Maximum torque (N.cm)	1.5 ± 0.2 1.5 [0.2] 1.3-1.9	1.3 ± 0.2 1.3 [0.2] 1.0-1.5	1.2 ± 0.3 1.3 [0.4] 0.8-1.6	1.3 ± 0.2 1.3 [0.3] 0.8-1.5	1.6 ± 0.3 1.5 [0.4] 1.2-2,4
	Angle of rotation (º)	546.9 ± 74.6 529.0 [137.3] 440.0-643.0	555.2 ± 80.2 593.0 [122.3] 430.0-648.0	699.0 ± 131.9 675.0 [87.3] 600.0-1047.0	622.3 ± 98.8 597.5 [123.5] 523.0-795.0	584.2 ± 95.4 611.0 [105.3] 431.0-722.0
Bending resistance	Maximum load (gf)	397.4 ± 32.4 400.5 [31.3] 344.0-437.0	325.9 ± 21.8 334.5 [33.3] 292.0-348.0	260.9 ± 20.4 261.5 [37.3] 233.0-289.0	357.7 ± 38.2 340.0 [60.0] 325.0-418.0	257.8 ± 18.3 262.0 [14.0] 227.0-282.0
Buckling resistance	Maximum load (gf)	286.7 ± 25.3 278.5 [36.0] 257.0-327.0	217.5 ± 20.4 222.5 [35.5] 185.0-242.0	174.4 ± 25.2 175.5 [42.5] 136.0-204.0	252.9 ± 20.2 245.0 [36.3] 231.0-282.0	280.5 ± 25.2 276.0 [42.3] 241.0-311.0
Cutting ability	Depth (mm)	7.1 ± 0.9 7.1 [1.1] 5.6-8.7	7.6 ± 0.7 7.7 [1.2] 6.7-8.5	4.5 ± 0.8 4.4 [1.0] 3.2-5.7	8.4 ± 1.0 8.5 [1.7] 7.0-9.8	7.0 ± 0.7 6.9 [0.9] 6.0-8.2

References

1. Martins JNR, Martins RF, Braz Fernandes FM, Silva EJNL. What meaningful information are the instruments mechanical testing giving us? A comprehensive review. J Endod 2022;48:985-1004.

2. Martins JNR, Silva EJNL, Marques D, Arantes-Oliveira S, Ginjeira A, Carames J, Braz Fernandes FM, Versiani MA. Multimethod assessment of design, metallurgical, and mechanical characteristics of original and counterfeit ProGlider instruments. Materials (Basel) 2022;15:3971.

3. Martins JNR, Silva EJNL, Marques D, Belladonna FG, Simoes-Carvalho M, da Costa RP, Ginjeira A, Braz Fernandes FM, Versiani MA. Comparison of five rotary systems regarding design, metallurgy, mechanical performance, and canal preparation-a multimethod research. Clin Oral Investig 2022;26:3299-310.

4. Martins JNR, Silva EJNL, Marques D, Pereira MR, Arantes-Oliveira S, Martins RF, Braz Fernandes FM, Versiani MA. Evaluation of design, metallurgy, microhardness, and mechanical properties of glide path instruments: a multimethod approach. J Endod 2021;47:1917-23.

5. Martins JNR, Silva EJNL, Marques D, Pereira MR, Ginjeira A, Silva RJC, Braz Fernandes FM, Versiani MA. Mechanical performance and metallurgical features of ProTaper Universal and 6 replicalike systems. J Endod 2020;46:1884-93.

6. Martins JNR, Silva EJNL, Baruwa AO, Pereira da Costa R, Braz Fernandes FM, Versiani MA. Comparative analysis of reciprocating and flat-side heat-treated rotary single-file systems: Design, metallurgical characteristics, and mechanical performance. Int Endod J 2023;56:896-908.

7. Martins JNR, Silva EJNL, Marques D, Belladonna F, Simoes-Carvalho M, Camacho E, Braz Fernandes FM, Versiani MA. Comparison of design, metallurgy, mechanical performance and shaping ability of replica-like and counterfeit instruments of the ProTaper Next system. Int Endod J 2021;54:780-92.

8. Martins JNR, Silva EJNL, Marques D, Belladonna F, Simoes-Carvalho M, Vieira VTL, Antunes HS, Braz Fernandes FMB, Versiani MA. Design, metallurgical features, mechanical performance and canal preparation of six reciprocating instruments. Int Endod J 2021;54:1623-37.

9. Silva EJNL, Martins JNR, Lima CO, Vieira VTL, Braz Fernandes FM, De-Deus G, Versiani MA. Mechanical tests, metallurgical characterization, and shaping ability of nickel-titanium rotary instruments: a multimethod research. J Endod 2020;46:1485-94.

10. Silva EJNL, Villarino LS, Vieira VT, Accorsi-Mendonca T, Antunes HD, De-Deus G, Lopes HP. Bending resistance and cyclic fatigue life of Reciproc, Unicone, and WaveOne reciprocating instruments. J Endod 2016;42:1789-93.

11. Silva EJNL, Ajuz NC, Martins JNR, Antunes BR, Lima CO, Vieira VTL, Braz-Fernandes FM, Versiani MA. Multimethod analysis of three rotary instruments produced by electric discharge machining technology. Int Endod J 2023;56:775-85.

12. Silva EJNL, Martins JNR, Ajuz NC, Antunes HS, Vieira VTL, Braz Fernandes FM, Belladonna FG, Versiani MA. A multimethod assessment of a new customized heat-treated nickel-titanium rotary file system. Materials (Basel) 2022;15:5288.

13. Silva EJNL, Martins JNR, Ajuz NC, Dos Santos Antunes H, Vieira VTL, Braz-Fernandes FM, Belladonna FG, Versiani MA. Design, metallurgy, mechanical properties, and shaping ability of 3 heat-treated reciprocating systems: a multimethod investigation. Clin Oral Investig 2023:doi: 10.1007/s00784-023-4899-2 [Online ahead of print].

14. Silva EJNL, Vieira VTL, Belladonna FG, Zuolo AS, Antunes HDS, Cavalcante DM, Elias CN, De-Deus G. Cyclic and torsional fatigue resistance of XP-endo Shaper and TRUShape instruments. J Endod 2018;44:168-72.

15. Silva EJNL, Vieira VTL, Hecksher F, Dos Santos Oliveira MRS, Dos Santos Antunes H, Moreira EJL. Cyclic fatigue using severely curved canals and torsional resistance of thermally treated reciprocating instruments. Clin Oral Investig 2018;22:2633-8.

16. Silva EJNL, Hecksher F, Antunes HDS, De-Deus G, Elias CN, Vieira VTL. Torsional fatigue resistance of blue-treated reciprocating instruments. J Endod 2018;44:1038-41.

17. International Organization for Standardization. ISO 3630-1. Dental root canal instruments: part 1-files, reamers, barbed broaches, rasps, paste carriers, explorers and cotton broaches. Geneva, Switzerland: International Organization for Standardization; 1992.

18. ASTM International. ASTM F2004−17: Standard test method for transformation temperature of nickel-titanium alloys by thermal analysis. West Conshohocken, PA: American Society for Testing and Materials; 2004.

19. Barbosa AFA, de Lima CO, Antunes BR, Sassone LM, Versiani MA, da Silva E. Effect of the progressive taper enlargement of buccal root canals of three-rooted maxillary molars: A stepwise micro-CT study. Aust Endod J 2023:doi: 10.1111/aej.12782 [Online ahead of print].

20. Versiani MA, Carvalho KKT, Martins JNR, Custodio ALN, Castro MAA, Akaki E, Silva-Sousa Y, Sousa-Neto MD. Effects of root canal enlargement on unprepared areas and coronal dentine thickness of three-rooted maxillary first premolars with different root configurations: A stepwise micro-CT study. Int Endod J 2022;55:1262-73.

21. Versiani MA, Carvalho KKT, Mazzi-Chaves JF, Sousa-Neto MD. Micro-computed tomographic evaluation of the shaping ability of XP-endo Shaper, iRaCe, and EdgeFile systems in long oval-shaped canals. J Endod 2018;44:489-95.

22. Versiani MA, Leoni GB, Steier L, De-Deus G, Tassani S, Pécora JD, Sousa Neto MD. Micro-CT study of oval-shaped canals prepared with SAF, Reciproc, WaveOne and ProTaper Universal systems. J Endod 2013;39:1060-6.

23. Zuolo ML, Zaia AA, Belladonna FG, Silva EJNL, Souza EM, Versiani MA, Lopes RT, De-Deus G. Micro-CT assessment of the shaping ability of four root canal instrumentation systems in oval-shaped canals. Int Endod J 2018;51:564-71.